

# Measurement of the depths at different regions of the anterior chamber in healthy Chinese adults

Yuan Zong<sup>1,2</sup>, Qing-Chen Li<sup>1,2</sup>, Huan Xu<sup>1,2</sup>, Jian Yu<sup>1,2</sup>, Chun-Hui Jiang<sup>1,2,3</sup>, Xing-Huai Sun<sup>1,2</sup>

<sup>1</sup>Department of Ophthalmology and Vision Science, Eye and ENT Hospital, Fudan University, Shanghai 200031, China

<sup>2</sup>Key Laboratory of Myopia of State Health Ministry, and Key Laboratory of Visual Impairment and Restoration of Shanghai, Shanghai 200031, China

<sup>3</sup>Department of Ophthalmology, Shanghai Fifth People's Hospital, Shanghai 200240, China

**Co-first authors:** Yuan Zong and Qing-Chen Li

**Correspondence to:** Chun-Hui Jiang. Department of Ophthalmology and Vision Science, Eye and ENT Hospital, Fudan University, 83 Fenyang Rd, Shanghai 200031, China. chhjiang70@163.com

Received: 2019-04-11 Accepted: 2019-07-08

**DOI:**10.18240/ijo.2020.01.20

**Citation:** Zong Y, Li QC, Xu H, Yu J, Jiang CH, Sun XH. Measurement of the depths at different regions of the anterior chamber in healthy Chinese adults. *Int J Ophthalmol* 2020;13(1):135-140

## INTRODUCTION

The anterior chamber depth (ACD) is of great interest to ophthalmologists, especially glaucoma specialists, because of its relationship to primary angle-closure glaucoma (PACG), which is responsible for nearly half of all cases of glaucoma-related blindness worldwide<sup>[1]</sup>. Several factors had been reported to play an important role in the increasing of PACG incidence with age<sup>[2]</sup>, including increases in lens vault (LV)<sup>[3]</sup>, lens thickness<sup>[4]</sup>, and iris curvature (IC)<sup>[5]</sup>. Monitoring all of these parameters could be difficult and time consuming. But, because all of these factors contribute to the pathogenesis of PACG *via* reductions in ACD, measuring the depths of different regions of the anterior chamber (AC) could be another alternative choice. However, in most prior studies, the ACD was only measured once along the optical axis<sup>[6-7]</sup>, so there is limited information on the ACDs of other regions of the AC. Cheon *et al*<sup>[8]</sup> reported that with the increasing in age, the angle opening distance at 500  $\mu$ m from the scleral spur (AOD500) decreases slower than the central ACD (AOD500: -0.00634 mm/y, central ACD: -0.02396 mm/y). Schuster *et al*<sup>[9]</sup> reported that the AC angle width was strongly associated with age whereas the central ACD was not. However, the variability of ACDs among different regions of the AC in normal subjects has not been determined. Here, we describe the use swept-source optical coherence tomography (OCT) to measure the ACDs in different regions of the AC, and to assess possible correlations of ACDs with age or gender.

## SUBJECTS AND METHODS

**Ethical Approval** This study was approved by the Institutional Review Board of the Eye and ENT Hospital of Fudan University, and was performed in accordance with the principles of the Declaration of Helsinki. All of the subjects signed informed consent forms.

**Subjects** Healthy Chinese adults were enrolled between May and July, 2015. All of the subjects underwent thorough ocular examinations, including measurement of best-corrected visual

## Abstract

• **AIM:** To measure the depths of different regions of the anterior chamber (AC) in healthy Chinese adults, and to explore possible correlations with age or gender.

• **METHODS:** The AC was imaged by swept-source optical coherence tomography in healthy Chinese adults. The horizontal scan of the right eye was used to measure the anterior chamber depth (ACD) at 199 points.

• **RESULTS:** A total of 309 images from 309 subjects were analyzed. The ACD values at nearly all locations were negatively correlated with age (all  $P < 0.05$ ), except for ACD1, 2, 198, and 199 (correspond to the iris roots). The mean annual decrease  $0.013 \pm 0.005$  mm/y for all ACDs combined,  $0.008 \pm 0.004$  mm/y for the peripheral region,  $0.017 \pm 0.003$  mm/y for the middle peripheral region, and  $0.014 \pm 0.001$  mm/y for the central region. The mean annual decrease was significantly different among these three regions ( $P < 0.001$ ). The ACD was greater in males than in females ( $P < 0.05$ ). The mean difference in ACD between males and females was  $0.081 \pm 0.025$  mm.

• **CONCLUSION:** This study showed that optical coherence tomography can be used to measure the ACD of different regions of the AC. We found reductions in ACD with age, although the reduction varied among different points, in healthy Chinese adults.

• **KEYWORDS:** optical coherence tomography; anterior chamber depth; age; gender; anterior chamber

acuity (BCVA); refraction measured by an auto-refraction system; spherical equivalent (SE), which was calculated as the spherical diopter (D) plus one-half of the cylindrical dioptric power; slit-lamp biomicroscopy; and undilated fundus examination by direct ophthalmoscopy. The axial length (AL) was measured using an IOL Master 500 (version 3.01; Carl Zeiss Meditec, Jena, Germany). Intraocular pressure (IOP) was measured using a non-contact tonometer (Topcon CT-80A Computerized Tonometer; Topcon, Tokyo, Japan). Subjects aged >18y were eligible if they met the following ocular criteria: BCVA $\geq$ 16/20, IOP $\leq$ 21 mm Hg, SE $\geq$ -3 D to  $\leq$ +1 D, AL 21-25 mm and pupil diameter 2-7 mm. Subjects who did not meet these ocular criteria, and those with histories of ocular surgery, ocular trauma, or intraocular disease, or a family history of glaucoma in a first-degree relative were excluded from this study.

**Swept-Source Optical Coherence Tomography Imaging and Analysis** OCT scans were obtained using a commercially available swept-source OCT (SS-OCT) system (CASIA SS-1000; Tomey Corporation, Nagoya, Japan; software version 6H.4), under normal room illumination (340 lx) without pupil dilation. An experienced observer (Zong Y) performed all image acquisitions. We used the standard anterior segment scan protocol, which produces a 3-dimensional scan of the anterior segment with 128 radial slices (each 6 mm in depth and 16 mm in length) in 2.4s. During analysis, the pupil diameter was automatically calculated using the system's built-in software. Using the central corneal thickness/ACD protocol, the central ACD was automatically calculated by the system after manually locating the two angle recesses.

**Measurements of Anterior Chamber Depths at 199 Locations** The horizontal (0°-180°) scans from the right eyes was selected for further analyses. Rhinoceros-NURBS Modeling for Windows (version 5.0; McNeel North America, Seattle, WA, USA) with the Grasshopper plug-in (McNeel North America) were used to measure the ACDs at 199 points (ACD1-199) with the following procedure. First, the boundary of the AC was drawn and the scale line from the OCT image was copied (Figure 1A). After removing the background bitmap, the outline of the AC was rotated to ensure both angle recesses were along one horizontal line (Figure 1B). Then, the image was recalibrated (Figure 1C) and two horizontal lines parallel to the line connecting both of the angle recesses were drawn above and below the outline of the AC (Figure 1D). The AC was then divided into 200 regions using an edited path in the Grasshopper plug-in (Figure 1E). ACD1 was defined as the length of the first vertical line between the superior and inferior boundaries of the AC from the temporal side (180°), ACD2 was defined as length of the second vertical line, and ACD3-199 were calculated in a similar way.

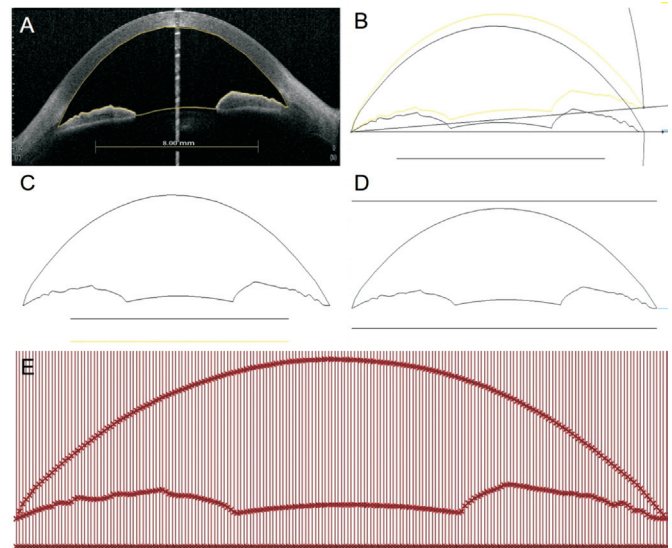


**Figure 1 Measurement of ACD at 199 points** A: The boundary of the AC was drawn and the scale line was copied from the OCT image; B: The background bitmap was removed and the outline of the AC was rotated to orientate both angle recesses along one horizontal line; C: The image was recalibrated; D: Two horizontal lines parallel to the line connecting the angle recesses were drawn above and below the outline of the AC; E: The AC was divided by placing 200 lines using a path created using the Grasshopper plug-in. ACD1-199 were defined from temporal (T) side (180°) to nasal (N) side (0°). ACD1 was defined as the length of the first vertical line from the T side, ACD2 was defined as length of the second vertical line, and the other ACDs were defined in the same way.

**Repeatability and Reproducibility** For the first 20 eyes, intra-observer repeatability was determined by one observer who manually measured ACD1-199 twice and inter-observer reproducibility was evaluated by two observers who each measured ACD1-199 independently.

**Statistical Analysis** Only the data from the right eyes was included in the final analysis. All analyses were performed using SPSS software version 16.0 (SPSS Inc., Chicago, IL, USA). Data are presented as the mean $\pm$ standard deviation (SD). Intra-class correlation coefficients (ICC) and Bland-Altman plots were used to assess the intra-observer repeatability and inter-observer reproducibility of ACD measurements. The agreement between the central ACD and ACD100 was assessed using ICCs and Bland-Altman plots. ICCs of 0.81-1.00 indicate almost perfect agreement and values of <0.40 indicate poor to fair agreement. Linear regression was used to analyze the associations between age, gender, and ACD1-199, and to determine the annual decrease in ACD. The annual reduction in ACD was calculated as the annual ACD reduction divided by the mean ACD. ACD1-199 were equally divided into three symmetrical regions: ACD1-33 and ACD167-199 (peripheral region); ACD34-66 and ACD134-166 (middle peripheral region); and ACD67-133 (central region). One-way analysis

**Table 1 Annual reductions in anterior chamber depths according to age**

ACD region	Mean±SD (mm/y)	Range (mm/y)	<i>P</i> <sup>a</sup>	<i>P</i> <sup>b</sup>
A	0.008±0.004	0.00002-0.014	<0.001 vs. B and C	<0.001
B	0.017±0.003	0.011-0.022	<0.001 vs. A and C	
C	0.014±0.001	0.013-0.017	<0.001 vs. B and C	

ACD: Anterior chamber depth; SD: Standard deviation; Region A: Peripheral region (ACD1-33 and ACD167-199); B: Middle region (ACD34-66 and ACD134-166); C: Central region (ACD67-133). <sup>a</sup>One-way analysis of variance followed by Bonferroni post-hoc tests; <sup>b</sup>*P* values from one-way analysis of variance for regions A, B, and C.

of variance (ANOVA) and Bonferroni's post-hoc test was used to compare the difference in reduction rates among the three different parts, and between pairs of region. The level of significance was set at *P*<0.05.

**RESULTS**

A total of 309 right eyes from 309 healthy Chinese adults (185 females and 124 males) with a mean±SD age of 36.48±9.51y (range: 18-65y) were analyzed in this study. Their mean IOP was 13.5±2.65 mm Hg (range: 7-21 mm Hg) and mean AL was 23.28±0.82 mm (range: 21.37-25.61 mm).

The intra-observer and inter-observer ICCs were >0.90 for all ACDs except for ACD1, 2, 198, and 199 (correspond to the iris roots) for which the ICCs were >0.8. Bland-Altman analysis also showed good intra-observer and inter-observer conformity. The mean central ACD was 2.89±0.32 mm (range: 1.56-3.81 mm) and the mean ACD100 was 2.86±0.32 mm (range: 1.56-3.36 mm). The ICC between the central ACD and ACD100 was 0.96, and Bland-Altman analysis showed good agreement between these values (Figure 2).

Linear regression analysis showed that all ACDs were negatively correlated with age (all *P*<0.05) except for ACD1, 2, 198, and 199 (*P*>0.05), which correspond to the iris roots. The mean annual decrease 0.013±0.005 mm/y for all ACDs combined, 0.008±0.004 mm/y for the peripheral region, 0.017±0.003 mm/y for the middle peripheral region, and 0.014±0.001 mm/y for the central region. The mean annual decrease was significantly different among these three regions, and between pairs of regions (all *P*<0.001, one-way ANOVA with Bonferroni post-hoc test; Table 1). The annual reduction was greatest in the middle peripheral region (Figure 3), especially around the iris collarettes (Figure 3B). The annual reductions in the ACDs in this region (ACD46-66 and ACD138-152) were >0.018 mm/y (mean annual reduction plus one SD: 0.013+0.005=0.018). The annual reduction rate of all ACDs was 0.763%±0.239%/y, and the angle recess regions (ACD8-27 and ACD182-193) presented relative greatest reduction rates (>1.002%/y, mean annual reduction rate plus one SD: 0.763%+0.239%=1.002%; Figure 4).

In additional analyses, we found that the majority (145/199) of ACDs were associated with gender (all *P*<0.05). The ACDs were significantly lower in females than in males, except for

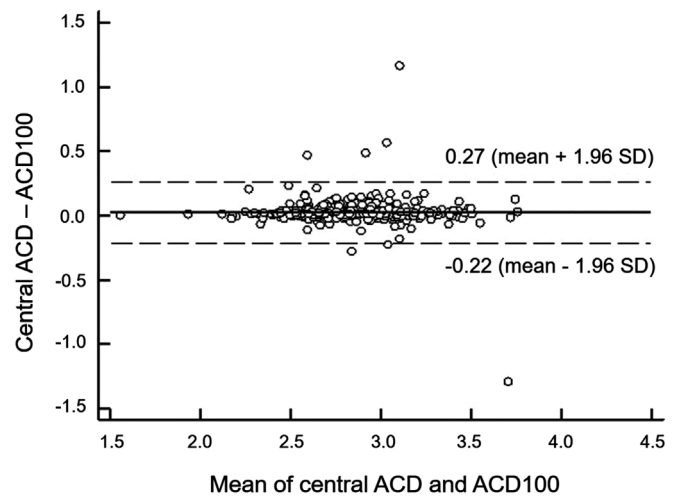


**Figure 2 Bland-Altman plot for assessing the agreement between the central ACD and the ACD at point 100.**

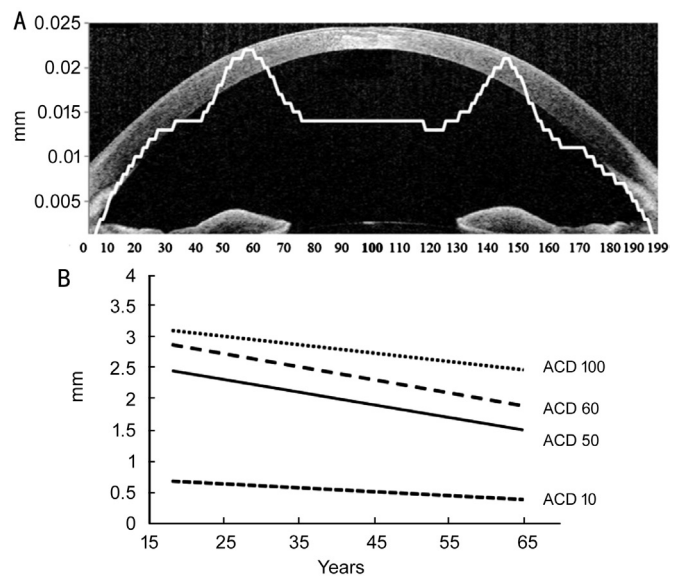


**Figure 3 Mean annual reductions (A) of ACD at points 1-199 and representative reduction sites of ACD (B).**

ACD1-3, ACD47-70, ACD131-153, and ACD196-199 (all *P*>0.05). These ACDs correspond to the angle recess and iris collarettes regions. The mean difference in ACD1-199 between males and females was 0.081±0.025 mm. The difference between males and females was greatest in the middle region of the iris (Figure 5), with differences in ACD21-41 and ACD160-166>0.106 mm (mean difference plus one SD: 0.081+0.025=0.106).

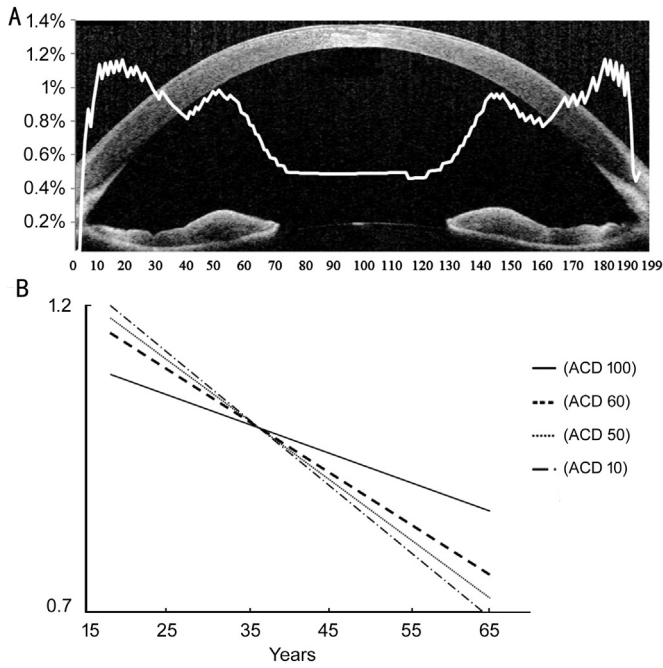


Figure 4 Mean annual reduction rates (A) of ACD at points 1-199 and representative reduction rates sites of ACD (B).

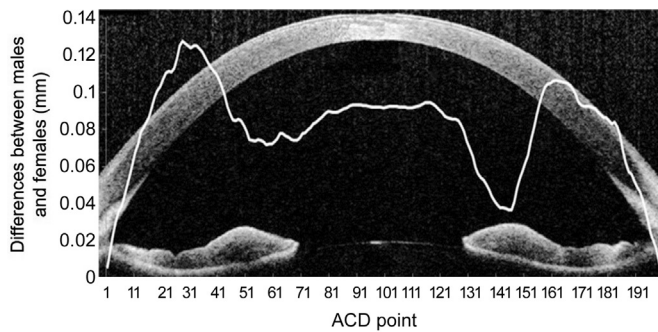


Figure 5 Differences in ACD at points 1-199 between males and females.

## DISCUSSION

In this study, we measured the depths of different regions of the AC, and determined their possible correlations with age and gender. We found that most of the ACDs were negatively correlated with age, but the annual reductions varied among different regions of the eye. The ACDs around the pupil margin showed the greatest annual reduction. The ACDs were significantly greater in males than in females for 145/199 points, especially in the middle region of the iris. To our knowledge, this is the first time to quantitative analysis of the AC at different regions, it could give insights to understand potentially mechanism of PACG, and guide us toward more effective diagnoses and treatments.

In prior studies, ACD was measured by A-scan ultrasonography<sup>[10]</sup>, optical biometry (IOL Master), Scheimpflug camera (Pentacam)<sup>[11]</sup>, ultrasound biomicroscopy, and OCT<sup>[12]</sup>. However, most of these studies focused on the central ACD. Notably, Ko *et al*<sup>[13]</sup> reported a poor correlation between the Van Herick grade and the central ACD. Kashiwagi *et al*<sup>[14]</sup>

reported that, in some patients with closed angle glaucoma, the peripheral ACD was correlated with elevated IOP, but central ACD was not. So evaluation of only the central ACD was not enough. On the other hand, study found that most of the PACG eyes had more than one mechanism underlying angle closure<sup>[15]</sup>, and it was crucial to reveal all the mechanisms for a better control of the IOP. And different mechanisms were related to the reduction of the ACD at different part of the AC for example pupillary block (PB) usually presents as a reduced depth of the central AC, while plateau iris (PI) configuration and thick peripheral iris roll are usually characterized by a relative deep central AC but a shallow peripheral AC<sup>[16-17]</sup>. Measuring the depths of different regions of the AC was first proposed by Tornquist<sup>[18]</sup> and the approach was modified by Hitchings *et al*<sup>[19]</sup>. But they determined the ratio between the peripheral and the axial chamber. Kashiwagi *et al*<sup>[20]</sup> developed another method that involved taking consecutive images under slit-lamp illumination but the intra-observer repeatability and inter-observer reproducibility deteriorated with increasing distance from the optical axis.

Here, we used a novel method to measure the ACD at 199 points. The intra-observer repeatability and inter-observer reproducibility of the method were good. The Bland-Altman plots showed good conformity and spatial accordance between the conventional central ACD and ACD100. Thus, the method used here could applied in future studies in which the ACDs are measured in different regions.

ACDs negatively correlated with age and female gender was in accordance with the findings that advancing age and female gender are two major predisposing factors for the development of PACG. Reductions in ACD with age have been reported. In our study, the annual reduction of ACD100 was 0.013 mm/y, which is similar to the previously reported reductions of 0.012 mm/y<sup>[21]</sup> and 0.024 mm/y<sup>[8]</sup>. The AC includes the posterior surface of the cornea and the anterior surfaces of the iris and lens. Previous studies demonstrated that the ACD is correlated with other ocular parameters, including IC<sup>[21]</sup>, lens thickness<sup>[22]</sup>, LV<sup>[23]</sup>, posterior corneal arc length<sup>[24]</sup>, AC width, lens thickness, and nuclear cataract grade<sup>[25]</sup>. Tan *et al*<sup>[23]</sup> reported that the LV increased with age, and might contribute to the greater reductions in ACDs of the middle and center of the AC. Sun *et al*<sup>[21]</sup> reported that the IC increased with age. We found greater annual reductions in ACDs in the middle peripheral region, at the highest point of the IC<sup>[26]</sup>, than in other regions. In the present study, the greatest annual reduction in ACD occurred around the iris collarettes, larger than >0.018 mm. Although the underlying reason is unclear, changes in iris thickness (IT) might contribute to the reduction in ACD in this region. Earlier studies of iris volume did not find a correlation between iris volume and age. Meanwhile, the results of studies

of IT were inconsistent. For example, Sun *et al*<sup>[21]</sup> reported that IT500 and IT750 were positively correlated with age but He *et al*<sup>[27]</sup> found a negative correlation between age and IT2000. Measuring the thicknesses of different regions of the iris might reveal whether there are differences in changes in IT between regions of the iris, and whether these changes contribute to the reduction in ACD with age.

Moreover, while most of the ACDs were negatively correlated with age, the annual reduction was higher around the iris collarettes at the pupil margin (Figure 3). On the other hand, although the annual reduction in the ACD was lower in the periphery than in the central area, the annual reduction percentage was on the contrary higher in the periphery than the center (Figure 4). And the progression over the years would actually lead to the angular closure found in elder subjects. The major mechanisms of PACG are categorized into four types based on anterior segment OCT findings: PB, PI configuration, thick peripheral iris roll, and exaggerated LV<sup>[28]</sup>. PB usually presents as a reduced depth of the whole AC, while PI configuration and thick peripheral iris roll are usually characterized by a relative deep central AC but a shallow peripheral AC. The greatest reductions in ACD with age were found at the AC angle and the pupil margin, was is consistent with the increasing incidence of PACG with age.

We also found that the ACDs of nearly all regions were less in females than in males, similar to the findings reported by Fernandez-Vigo *et al*<sup>[29]</sup>. This also agrees with our clinical experience that the prevalence of PACG is higher in females than in males. The differences in ACDs between males and females were most pronounced at ACD21-41 and ACD160-166 (all >0.106 mm), which correspond to the middle region of the iris. These findings are also consistent with the higher prevalence of PI in females<sup>[30]</sup>.

Some limitations of our study include its cross-sectional design, the analysis of horizontal scans only and as only subjects from 18 to 65 years old were included in the study, the annual reduction of ACD at subjects over 65y was not known. In following study, PACG patients with PI configuration or PB will included, and ACD at different regions will be compared to find a valuable way in differentiating PB and PI configuration. In conclusion, we successfully used SS-OCT to reliably and reproducibly measure the depths of different regions of the AC. We found reductions in ACDs with age, although the reductions were not uniform throughout the AC, and the greatest reductions in ACD occurred in the region around the iris collarettes.

#### ACKNOWLEDGEMENTS

The authors thank the subjects and our colleagues who helped perform this study.

**Foundations:** Supported by research grants from the National Key R&D Program of China (No.2017YFC0108200); the Shanghai Committee of Science and Technology (No.16140901000; No.13430710500; No.15DZ1942204).

**Conflicts of Interest:** Zong Y, None; Li QC, None; Xu H, None; Yu J, None; Jiang CH, None; Sun XH, None.

#### REFERENCES

- 1 Quigley HA, Broman AT. The number of people with glaucoma worldwide in 2010 and 2020. *Br J Ophthalmol* 2006;90(3):262-267.
- 2 Sun X, Dai Y, Chen Y, Yu DY, Cringle SJ, Chen J, Kong X, Wang X, Jiang C. Primary angle closure glaucoma: what we know and what we don't know. *Prog Retin Eye Res* 2017;57:26-45.
- 3 Zhang Y, Li SZ, Li L, He MG, Thomas R, Wang NL. Dynamic iris changes as a risk factor in primary angle closure disease. *Invest Ophthalmol Vis Sci* 2016;57(1):218-226.
- 4 Nongpiur ME, He M, Amerasinghe N, Friedman DS, Tay WT, Baskaran M, Smith SD, Wong TY, Aung T. Lens vault, thickness, and position in Chinese subjects with angle closure. *Ophthalmology* 2011;118(3):474-479.
- 5 Moghimi S, Torkashvand A, Mohammadi M, Yaseri M, Saunders LJ, Lin SC, Weinreb RN. Classification of primary angle closure spectrum with hierarchical cluster analysis. *PLoS One* 2018;13(7):e0199157.
- 6 Zhang J, Ni Y, Li P, Sun W, Liu M, Guo D, Du C. Anterior segment biometry with phenylephrine and tropicamide during accommodation imaged with ultralong scan depth optical coherence tomography. *J Ophthalmol* 2019;2019:6827215.
- 7 Kamiya K, Shimizu K, Igarashi A, Kitazawa Y, Kojima T, Nakamura T, Ichikawa K. Posterior chamber phakic intraocular lens implantation in eyes with an anterior chamber depth of less than 3 mm: a multicenter study. *Sci Rep* 2018;8(1):13322.
- 8 Cheon MH, Sung KR, Choi EH, Kang SY, Cho JW, Lee S, Kim JY, Tchah HW, Kook MS. Effect of age on anterior chamber angle configuration in Asians determined by anterior segment optical coherence tomography; clinic-based study. *Acta Ophthalmologica* 2010;88(6):e205-210.
- 9 Schuster AK, Pfeiffer N, Nickels S, Schulz A, Höhn R, Wild PS, Binder H, Münzel T, Beutel ME, Vossmerbaeumer U. Distribution of anterior chamber angle width and correlation with age, refraction, and anterior chamber depth: the gutenber health study. *Invest Ophthalmol Vis Sci* 2016;57(8):3740-3746.
- 10 Hashemi H, Yazdani K, Mehravaran S, Fotouhi A. Anterior chamber depth measurement with a-scan ultrasonography, Orbscan II, and IOLMaster. *Optom Vis Sci* 2005;82(10):900-904.
- 11 Nakakura S, Mori E, Nagatomi N, Tabuchi H, Kiuchi Y. Comparison of anterior chamber depth measurements by 3-dimensional optical coherence tomography, partial coherence interferometry biometry, Scheimpflug rotating camera imaging, and ultrasound biomicroscopy. *J Cataract Refract Surg* 2012;38(7):1207-1213.
- 12 Kucumen RB, Yenerel NM, Gorgun E, Kulacoglu DN, Dinc UA, Alimgil ML. Anterior segment optical coherence tomography measurement of anterior chamber depth and angle changes after

- phacoemulsification and intraocular lens implantation. *J Cataract Refract Surg* 2008;34(10):1694-1698.
- 13 Ko YC, Liu CJ, Hsu WM, Cheng CY, Kuang TM, Chou P. Determinants and characteristics of angle-closure disease in an elderly Chinese population. *Ophthalmic Epidemiol* 2015;22(2):109-115.
- 14 Kashiwagi K, Furuya T, Kashiwagi F. Changes in peripheral anterior chamber depth of a case of relapsing polychondritis with recurrent secondary angle closure glaucoma section sign. *Open Ophthalmol J* 2008;2(1):1-4.
- 15 Mizoguchi T, Ozaki M, Wakiyama H, Ogino N. Plateau iris in Japanese patients with primary angle closure and primary angle closure glaucoma. *Clin Ophthalmol* 2015:1159-1163.
- 16 Mandell MA, Pavlin CJ, Weisbrod DJ, Simpson ER. Anterior chamber depth in Plateau iris syndrome and pupillary block as measured by ultrasound biomicroscopy. *Am J Ophthalmol* 2003; 136(5):900-903.
- 17 Chen YY, Chu D, Chou P. Enhancing the early differential diagnosis of plateau iris and pupillary block using a-scan ultrasonography. *PLoS One* 2015;10(2):e0118811.
- 18 Tornquist R. Peripheral chamber depth in shallow anterior chamber. *Br J Ophthalmol* 1959;43(3):169-176.
- 19 Hitchings RA, Romano J, Clark P. Measurements of axial and peripheral anterior chamber depth: accuracy of a photographic method. *Br J Ophthalmol* 1984;68(3):212-214.
- 20 Kashiwagi K, Kashiwagi F, Toda Y, Osada K, Tsumura T, Tsukahara S. A newly developed peripheral anterior chamber depth analysis system: principle, accuracy, and reproducibility. *Br J Ophthalmol* 2004;88(8):1030-1035.
- 21 Sun JH, Sung KR, Yun SC, Cheon MH, Tchah HW, Kim MJ, Kim JY. Factors associated with anterior chamber narrowing with age: an optical coherence tomography study. *Invest Ophthalmol Vis Sci* 2012;53(6):2607-2610.
- 22 Praveen MR, Vasavada AR, Shah SK, Shah CB, Patel UP, Dixit NV, Rawal S. Lens thickness of Indian eyes: impact of isolated lens opacity, age, axial length, and influence on anterior chamber depth. *Eye* 2009;23(7):1542-1548.
- 23 Tan GS, He M, Zhao W, Sakata LM, Li J, Nongpiur ME, Lavanya R, Friedman DS, Aung T. Determinants of lens vault and association with narrow angles in patients from Singapore. *Am J Ophthalmol* 2012;154(1):39-46.
- 24 Sng CC, Foo LL, Cheng CY, Allen JC, He M, Krishnaswamy G, Nongpiur ME, Friedman DS, Wong TY, Aung T. Determinants of anterior chamber depth: the Singapore Chinese eye study. *Ophthalmology* 2012;119(6):1143-1150.
- 25 Jonas JB, Nangia V, Gupta R, Khare A, Sinha A, Agarwal S, Bhate K. Anterior chamber depth and its associations with ocular and general parameters in adults. *Clin Exp Ophthalmol* 2012;40(6):550-556.
- 26 Sng CC, Allen JC, Nongpiur ME, Foo LL, Zheng Y, Cheung CY, He M, Friedman DS, Wong TY, Aung T. Associations of iris structural measurements in a Chinese population: the Singapore Chinese eye study. *Invest Ophthalmol Vis Sci* 2013;54(4):2829-2835.
- 27 He Y, Baskaran M, Narayanaswamy AK, Sakata LM, Wu R, Liu D, Nongpiur ME, He M, Friedman DS, Aung T. Changes in anterior segment dimensions over 4 years in a cohort of Singaporean subjects with open angles. *Br J Ophthalmol* 2015;99(8):1097-1102.
- 28 Shabana N, Aquino MC, See J, Ce Z, Tan AM, Nolan WP, Hitchings R, Young SM, Loon SC, Sng CC, Wong W, Chew PT. Quantitative evaluation of anterior chamber parameters using anterior segment optical coherence tomography in primary angle closure mechanisms. *Clin Exp Ophthalmol* 2012;40(8):792-801.
- 29 Fernández-Vigo JI, Fernández-Vigo JÁ, Macarro-Merino A, Fernández-Pérez C, Martínez-de-la-Casa JM, García-Feijóo J. Determinants of anterior chamber depth in a large Caucasian population and agreement between intra-ocular lens Master and Pentacam measurements of this variable. *Acta Ophthalmol* 2016;94(2):e150-e155.
- 30 Mansoori T, Sarvepally VK, Balakrishna N. Plateau iris in primary angle closure glaucoma: an ultrasound biomicroscopy study. *J Glaucoma* 2016;25(2):e82-e86.